Table S1. Binding of select IgG samples to human FCRL3, CD16A and CD32B/C by Biacore.

Protein on sensor	Ig sample [1]	KD (μM) [2]	Binding model
FCRL3	#1 IgG1	No binding	-
FCRL3	#2 IgG2	No binding	-
FCRL3	#3 IgG3	Weak binding [3]	-
FCRL3	#4 IgG4	No binding	-
FCRL3	IgG-Fc	No binding	-
FCRL3	IgG-F(ab')$_2$	No binding	-
CD16A	#1 IgG1	3.6	Steady-state
CD16A	IgG-Fc	3.5	Steady-state
CD16A	IgG-F(ab')$_2$	No binding	-
CD16A	IVIg with SA [4]	2.7	Steady-state
CD16A	IVIg lacking SA	4.6	Steady-state
CD32B/C	#1 IgG1	12.9	Steady-state
CD32B/C	IgG-Fc	7.2	Steady-state
CD32B/C	IgG-F(ab')$_2$	No binding	-
CD32B/C	IVIg with SA	8.0	Steady-state
CD32B/C	IVIg lacking SA	10.0	Steady-state

[1] Numbering of full IgG samples follows that in Table 1.

[2] With CD16A and CD32B/C, KD was determined using steady-state analysis, due to the fast kinetics.

[3] Due to weak binding, KD could not be reliably established.

[4] SA, sialic acid.

SUPPLEMENTAL FIGURE LEGENDS

Fig. S1. Binding of additional IgG samples to recombinant FCRL5.

Representative binding curves are shown for samples 5-18 (Table 1). Biacore was performed as indicated under Fig. 1. KD values are shown, in parenthesis indicating FCRL5 densities on the sensor in relative units. The y-axes are scaled to allow assessment of details, and are not proportional to FCRL5 density.

Fig. S2. Binding of IgG samples at an additional FCRL5 density, or using alternate data fits.

Biacore was performed as indicated under Fig. 1. (A) For samples 1-4 (Table 1), the same binding curves shown on Fig. 1a were fitted using 1:1 binding model. KD values are not provided, as fits were poor. (B) Representative binding of samples 2 and 4 (Table 1) is shown at FCRL5 densities (indicated in parenthesis) different from those shown on Fig. 1. Fits were obtained using two-state binding model for sample 2; 1:1 binding model for sample 4.

Fig. S3. Sample purities assessed by protein staining and Western blotting.

(A,B) Purities of recombinant FCRL5-His (1 µg protein) and modified IgG samples (2 µg protein) used in Biacore studies shown on Fig. 4 were assessed by non-reduced and reduced SDS-PAGE analysis, followed by protein staining. (B) Purification of the IgG1-Fab-Fc fragment is shown. On the left, fractions from the second Superdex200 column were assessed by non-reduced SDS-PAGE analysis, followed by protein staining, indicating the identity of bands (see *Materials and Methods* for details). On the right, purity of the final IgG1-Fab-Fc fragment used

in Biacore studies. (C) Sialic acid content of IVIg samples (1 µg protein) eluted from or not binding to (flow through) *Sambucus nigra* agglutinin column was assessed by Western blot analysis (using reduced SDS-PAGE), blotting with *Sambucus nigra* agglutinin. Note that slower mobility of the H-chain in the eluted samples likely reflects differences in glycosylation.

Fig. S1

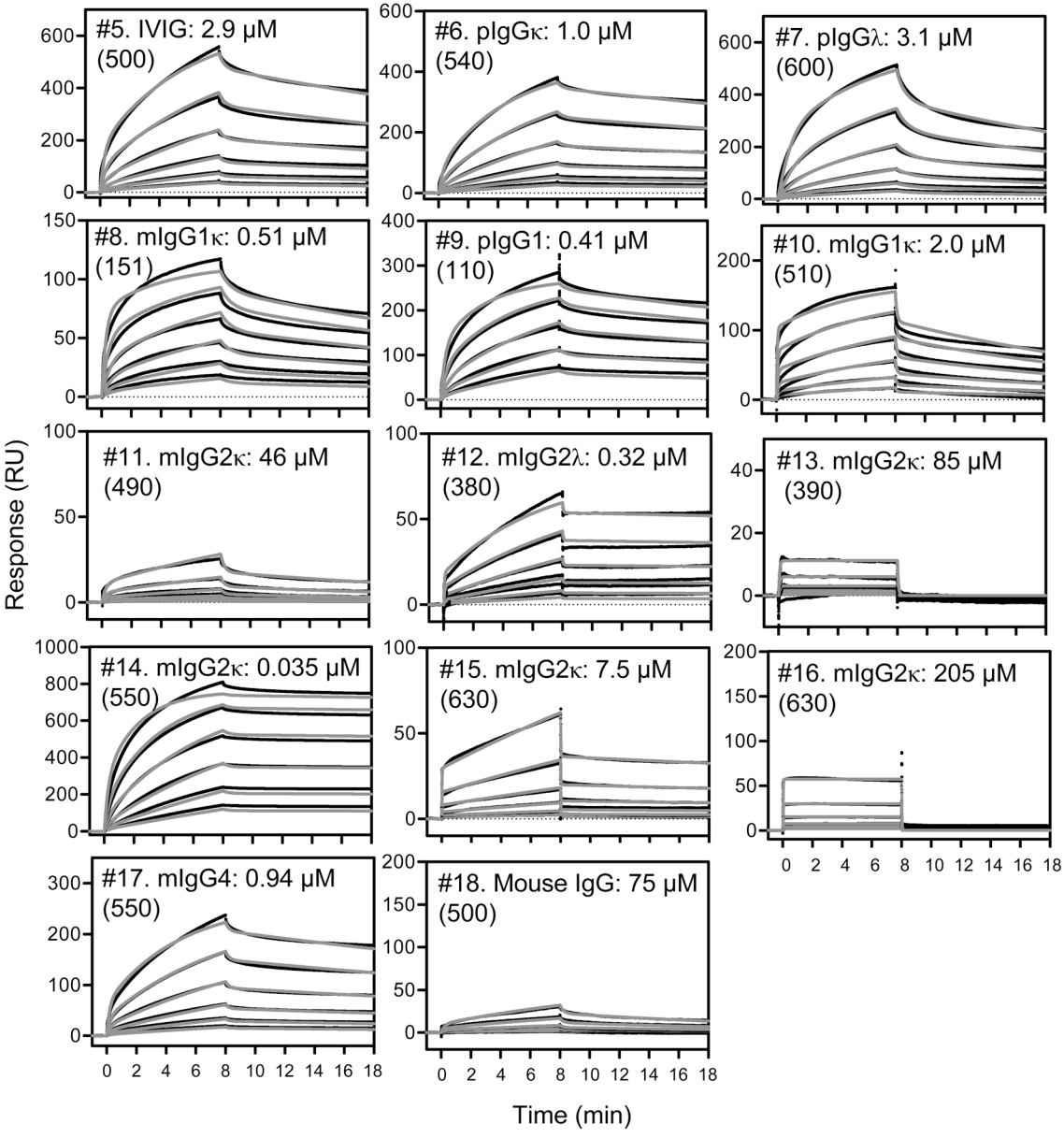
#5. IVIG: 2.9 μM (500)
#6. pIgGκ: 1.0 μM (540)
#7. pIgGλ: 3.1 μM (600)
#8. mIgG1κ: 0.51 μM (151)
#9. pIgG1: 0.41 μM (110)
#10. mIgG1κ: 2.0 μM (510)
#11. mIgG2κ: 46 μM (490)
#12. mIgG2λ: 0.32 μM (380)
#13. mIgG2κ: 85 μM (390)
#14. mIgG2κ: 0.035 μM (550)
#15. mIgG2κ: 7.5 μM (630)
#16. mIgG2κ: 205 μM (630)
#17. mIgG4: 0.94 μM (550)
#18. Mouse IgG: 75 μM (500)
Response (RU)
Time (min)

Fig. S2

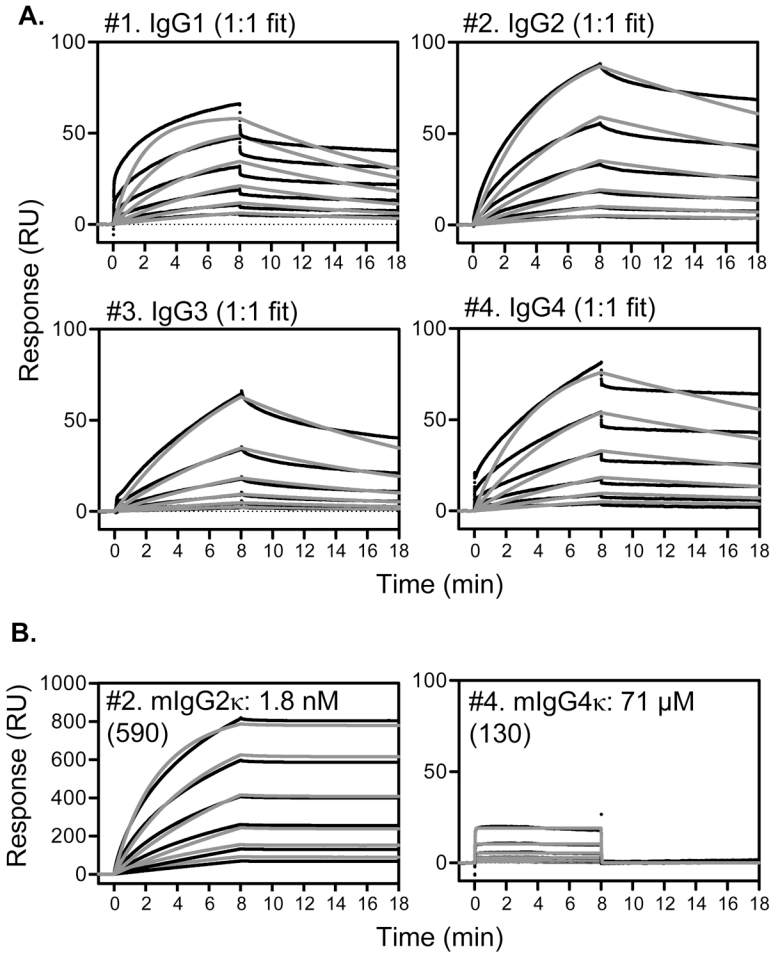
A.
#1. IgG1 (1:1 fit)
#2. IgG2 (1:1 fit)
#3. IgG3 (1:1 fit)
#4. IgG4 (1:1 fit)
Response (RU)
Time (min)
B.
#2. mIgG2κ: 1.8 nM
(590)
#4. mIgG4κ: 71 μM
(130)
Response (RU)
Time (min)

Fig. S3.

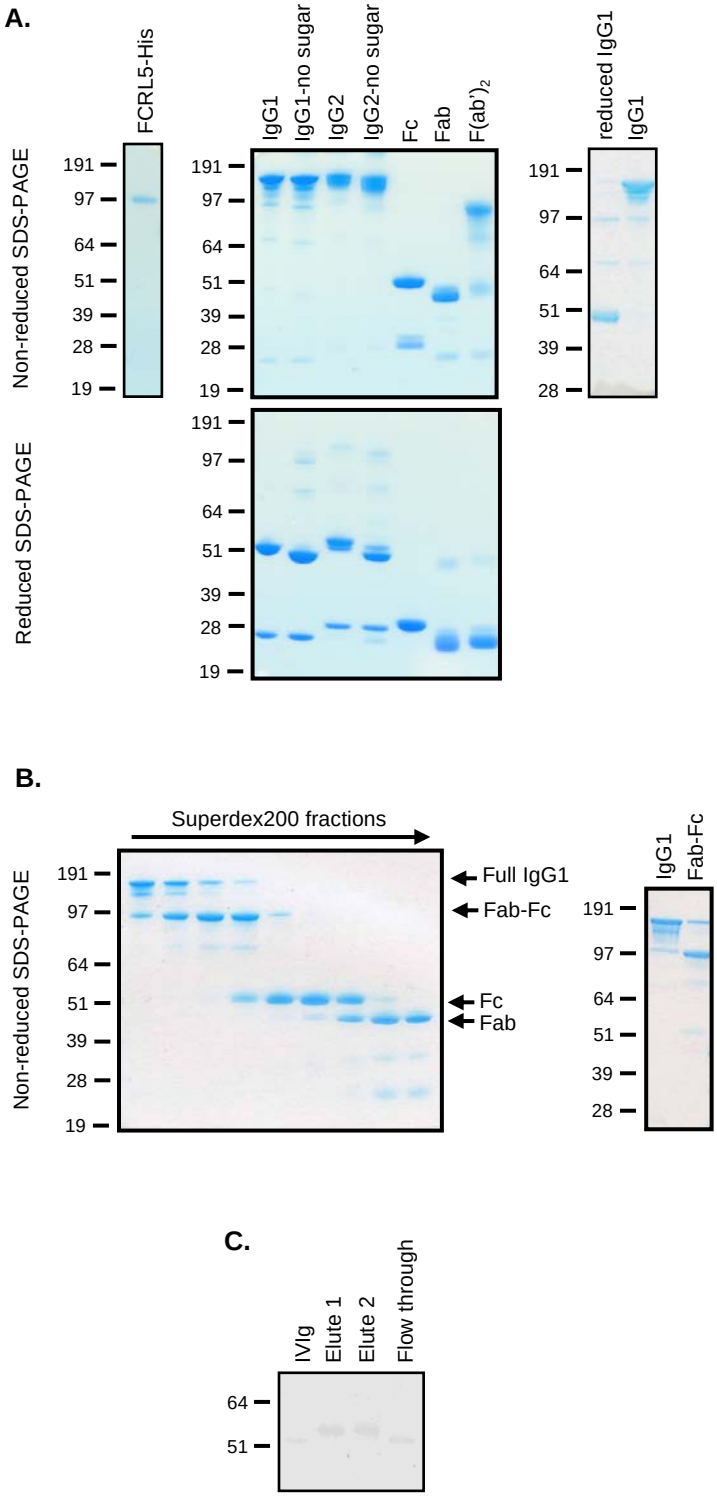
A.
Non-reduced SDS-PAGE
Reduced SDS-PAGE
FCRL5-His
IgG1
IgG1-no sugar
IgG2
IgG2-no sugar
Fc
Fab
F(ab')2
reduced IgG1
IgG1
191
97
64
51
39
28
19
B.
Superdex200 fractions
Non-reduced SDS-PAGE
Full IgG1
Fab-Fc
Fc
Fab
IgG1
Fab-Fc
C.
IVIg
Elute 1
Elute 2
Flow through
64
51